

Two-Dimensional Numerical Simulations

Motivation of these simulations was to observe instabilities of fluid flowing down a vertical and down an inclined ($\alpha = \frac{\pi}{4}$) plane. We predominantly focused on three types of wave profiles: stable traveling wave solution, convective instability and absolute instability.

Governing equation and numerical method

For two dimensional simulations, equation governing the film height is considered as follows [1]:

$$h_t + [h^3(C h_{xxx} - B h_x) + \mathcal{N}(m^2 - h m m') h_x + u h^3]_x = 0 \quad (1)$$

$$m(h) = \frac{h^{\frac{3}{2}}}{\beta^{\frac{3}{2}} + h^{\frac{3}{2}}}$$

where β measures the film height over which anchoring adjusts from strong to weak, in our simulations $\beta = 1$ is used. Numerical solution is obtained using finite difference method. Precisely, implicit Crank–Nicolson method in time, second order discretization in space and Newton's method are implemented [2]. Constant flux boundary condition is used at the inlet and prewetting condition at the contact line, also called precursor film:

$$\begin{aligned} h(0, t) &= 1, & h_x(0, t) &= 0 \\ h(L, t) &= b, & h_x(L, t) &= 0, \end{aligned}$$

where b is the precursor thickness, here $b = 0.1$ is used. The initial condition is chosen as a hyperbolic tangent to connect smoothly $h = 1$ and $h = b$ at $x = x_f$. [3] For these simulations $x_f = 40$.

Figure 1. Flow down the vertical plane (N=16). From top to bottom, t=0, 40, 80, 120.

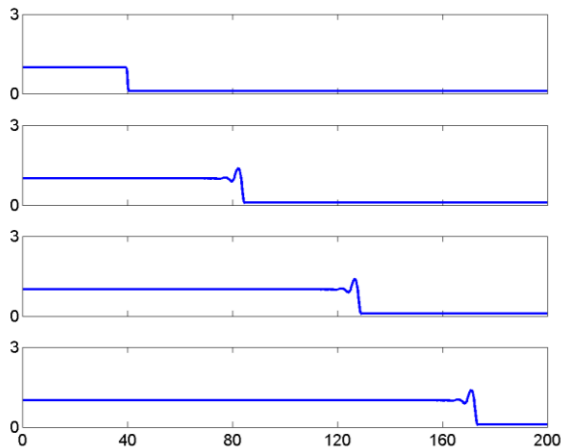
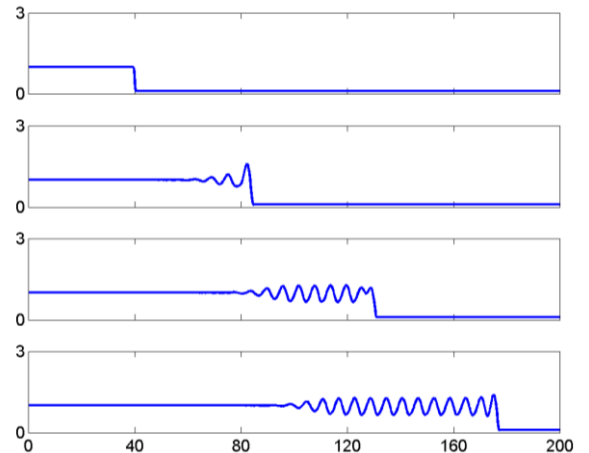


Figure 2. Convective instability N=22 for flow down the vertical. From top to bottom, t=0, 40, 80, 120.



Numerical Results for $\alpha = \frac{\pi}{2}$

By varying parameter \mathcal{N} and keeping other parameters constant, we obtained a range of \mathcal{N} for each of the desired wave profiles mentioned above.

Stable traveling wave solution: $0 < \mathcal{N} < 18.6$. For this range of \mathcal{N} the dominant capillary ridge is present, followed by a secondary strongly damped oscillation. Figure 1 shows wave profile for $\mathcal{N} = 16$ at different times. For $t > 3$ we observe a traveling wave solution with a constant velocity which agrees with the result obtained from linear stability analysis ($U = (1 + b + b^2)u$).

Convective instability: $18.6 \leq \mathcal{N} < 24.4$. These instabilities are characterized by sinusoidal waves followed by a constant state. Figure 2 illustrates $\mathcal{N} = 22$ wave profile. Capillary ridge is still dominant. However, since the waves are moving faster than the front, as the first wave reaches the front, it interacts and merges with it. As the front moves forward its height decreases until the next wave arrives. Therefore the velocity of the front is not constant anymore.[3]

Absolute instability: $24.4 \leq \mathcal{N}$. For early times we still observe flat film which disappears after sufficiently long time. Figure 3 shows wave profile for $\mathcal{N} = 27$. Also two kinds of waves are present, sinusoidal waves and solitary type waves.

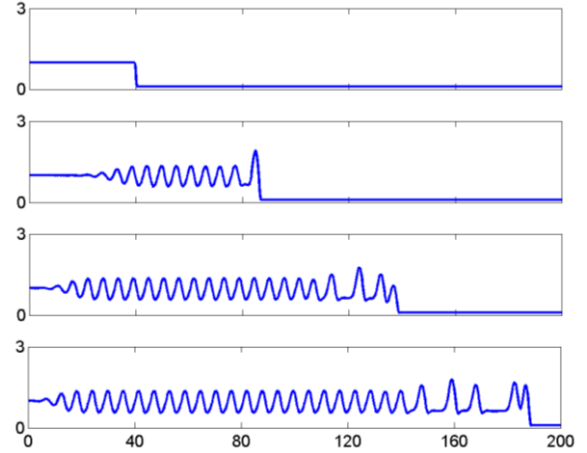


Figure 3. Flow down the vertical plane ($N=27$). From top to bottom, $t=0, 40, 80, 120$.

Finding critical values of \mathcal{N} from LSA

To find the value of \mathcal{N} where the transition occurs from stability to convective instability (\mathcal{N}_{c1}) and from convective to absolute instability (\mathcal{N}_{c2}) we will study the speed of the boundary of the expanding wave packet. Let us consider the governing equation (1) again. It follows from linear stability analysis by assuming $h = 1 + \varepsilon h_1$:

$$h_{1t} + Ch_{1xxxxx} - Bh_{1xxx} + \mathcal{N} \left(\frac{1 - \beta^{\frac{3}{2}}}{(\beta^{\frac{3}{2}} + 1)^3} \right) h_{1xx} + 3uh_{1x} = 0.$$

Substituting $h \sim e^{i(kx - \omega t)}$, where $\omega = \omega_r + i\omega_i$ we obtain the dispersion relation

$$-i\omega_r + \omega_i + \mathcal{C}k^4 + \mathcal{B}k^2 - \mathcal{N} \left(\frac{1 - \beta^{\frac{3}{2}}}{(\beta^{\frac{3}{2}} + 1)^3} \right) k^2 + i3uk = 0$$

Hence

$$\omega_r = 3uk \quad \omega_i = - \left(\mathcal{C}k^4 - \left(\mathcal{B} - \mathcal{N} \left(\frac{1 - \beta^{\frac{3}{2}}}{(\beta^{\frac{3}{2}} + 1)^3} \right) \right) k^2 \right)$$

It has been found that the speed of the left and right boundary of the wave packet [3] is given as

$$\left(\frac{x}{t} \right)_{\pm} = 3u \pm 1.62 \left(-\mathcal{B} + \mathcal{N} \left(\frac{1 - \beta^{\frac{3}{2}}}{(\beta^{\frac{3}{2}} + 1)^3} \right) \right)^{\frac{3}{2}}$$

In the case of $\alpha = \frac{\pi}{2}$ we have $\mathcal{C} = 1$, $\mathcal{B} = 0$, $u = 1$ and $\beta = 1$ we have $\left(\frac{x}{t} \right)_{\pm} = 3 \pm 1.62 \left(\frac{\mathcal{N}}{16} \right)^{\frac{3}{2}}$. We can see that the right moving boundary $\left(\frac{x}{t} \right)_{+}$ is always positive and greater than the speed of leading capillary ridge. This explains why waves catch up and merge with the front. The left moving boundary will determine which kind of wave profile will appear. If the speed of the left boundary, $\left(\frac{x}{t} \right)_{-}$, is positive, then that boundary will move to the right. However, if it is slower than the front ($U = 1 + b + b^2$), the region with sinelike waves will still grow, but there will always be a constant state region. Therefore, we will have convective instability for the following region:

$$0 < 3 - 1.62 \left(\frac{\mathcal{N}}{16} \right)^{\frac{3}{2}} < 1.11.$$

Solving for \mathcal{N} yields $17.79 < \mathcal{N} < 24.13$. Comparison with numerical results is given in Table 1. We can see that the results agree within 5% error.

Results for $\alpha = \frac{\pi}{4}$

Using the inclination angle $\frac{\pi}{4}$, produced similar results. The parameters in this case are $\mathcal{C} = 1$, $\mathcal{B} = \frac{\sqrt{2}}{2}$, $u = \frac{\sqrt{2}}{2}$ and $\beta = 1$. Numerical and analytical values for \mathcal{N}_{c1} and \mathcal{N}_{c2} are given in Table I. Again, we see a very good agreement.

Table 1

	$\alpha = \frac{\pi}{2}$		$\alpha = \frac{\pi}{4}$	
	Num	LSA	Num	LSA
\mathcal{N}_{c1}	18.6	17.79	25.43	25.44
\mathcal{N}_{c2}	24.4	24.13	30.6	30.46

NUMERICS

Back ground:

Numerical methods must be applied to this equation to obtain numerical solutions. For our simulations, we needed a method to solve to solve a PDE with either two or three variables. The general equation which models the height of a drop of liquid crystal is given by

$$h_t + C \nabla \cdot [h^3 \nabla \nabla^2 h] - B \nabla \cdot [h^3 \nabla h] + N \nabla \cdot [(m^2 - h m m') \nabla h] + U \frac{\partial h^3}{\partial x} = 0 \quad (1)$$

In order to solve this equation numerically, the terms had to first be discretized. This discretization was accomplished by applying a **centered finite difference based computational technique** on the terms of the PDE. The way in which the equation was solved is summed up in the steps outlined below. For simplicity, the scheme is shown for the two dimensional case, but can be directly extended to three dimensions by repeating the steps for the additional space component. In two dimensions, the equation (1) above reduces to

$$h_t + C \frac{\partial}{\partial x} [h^3 h_{xxx}] - B \frac{\partial}{\partial x} [h^3 h_x] + N \frac{\partial}{\partial x} [(m^2 - h m m') h_x] + U \frac{\partial h^3}{\partial x} = 0 \quad (2)$$

The finite difference discretization procedure for this case is as follows:

Spatial discretization:

1. Discretization of the surface tension term: The surface tension term is given by

$$h_t = (g(h) h_{xxx})_x \quad (3)$$

(Where $g(h) = h^3$). We defined the forward and backward differences by

$$y_{x,i} = \frac{y_{i+1} - y_i}{\Delta x}, \quad y_{\bar{x},i} = \frac{y_i - y_{i-1}}{\Delta x} \quad (4)$$

The surface tension term (3) was thus discretized as

$$y_{i,t} = (a(y_{i-1}, y_i) y_{\bar{x}x\bar{x},i})_x \quad (5)$$

Where $a(s_1, s_2)$ is some approximation to $g(h)$. This scheme produces a five point stencil in the 2D case (two points on either side of the given point i on one axis) and a nine point stencil in the 3D case (two points on either side of the given point i on each axis).

2. Discretization of the gravity term:

The normal component of gravity term given by $\frac{\partial}{\partial x} [h^3 h_x]$ was discretized using the centered finite difference, and is expressed as

$$\left(\frac{\partial}{\partial x} h^3 h_x \right)_i \approx \frac{1}{\Delta x^2} (a(y_{i+1}, y_i) y_{x,i})_{\bar{x}} \quad (6)$$

This scheme produces a three point stencil in the 2D case and a five point stencil in the 3D case.

The parallel component of gravity term given by $\frac{\partial h^3}{\partial x}$ was discretized as

$$\left(\frac{\partial h^3}{\partial x} \right)_i \approx \frac{1}{2\Delta x} (y_{i+1}^3 - y_{i-1}^3) \quad (7)$$

The weak anchoring term was also discretized using the centered finite difference method.

Time discretization: An implicit scheme was used to carry out the time discretization. The scheme used is a θ scheme, and the PDE is discretized as follows

$$\frac{y_i(t+\Delta t) - y_i(\Delta t)}{\Delta t} = \theta f_i(t) + (1 - \theta) f_i(t + \Delta t), \quad i = 1, \dots, N_x - 1 \quad (8)$$

Where $0 < \theta < 1$, and f_i is the discretization of the spatial terms of equation (1). The specific θ scheme used is that for which $\theta = 1/2$, the implicit second-order Crank- Nicholson scheme.

The result of the Crank-Nicholson scheme is a system of $N_x - 1$ nonlinear algebraic equations for $y_i(t + \Delta t), i = 1, \dots, N_x - 1$ where N_x represents the number of grid points used. These nonlinear equations were linearized using Newton's method: Newton's method is used first to linearize equation (8) about a guess for the solution, and then solve the resulting linear system for the correction. These iterations are repeated until the convergence criterion is met.

Our simulations:

In this project, we ran 3D liquid crystal simulations using the programming language FORTRAN. We ran these for two different cases:

1. Constant Flux: We ran the simulation for the hypothetical case where an infinite volume of liquid is used. In this case, the initial condition used is the semi-infinite hyperbolic tangent profile. The analysis carried out on this simulation was compared to the analysis carried out on equation (2).
2. Constant Volume: We also ran simulation for the case where a fixed volume of liquid is used. In this case, the initial condition used was a square hyperbolic tangent profile. This simulation served to model the experiments which we carried out.

Both of these simulations are shown in the graphs below. In both cases, the parameters used were: $C = 1, B = 0, N = 10, U = 1, b = 0.1, \beta = 1$. These parameters indicate a liquid crystal flowing down a vertical surface (at a 90 degree angle). We ran these simulations for 10 time steps, and obtained an output files at each time step. The output files were then plotted and analyzed using MATLAB. For each case, we sought to find out the wave length k with the maximum growth rate σ . To this end, we ran simulations for $k = 6, 8, 10, 12, 14, 16, 18$ and 20 . We carried out growth rate analysis on the results of these simulations, and the results are shown below.

Lastly, we ran a simulation for a liquid crystal flowing down an incline, as done by the experimental group. For this, we used the following parameters: $C = 1, B = 1/\sqrt{2}, N = 30, U = 1/\sqrt{2}$, and the wave length $k = 14$ (which we found to be the critical wave length for this case).

References

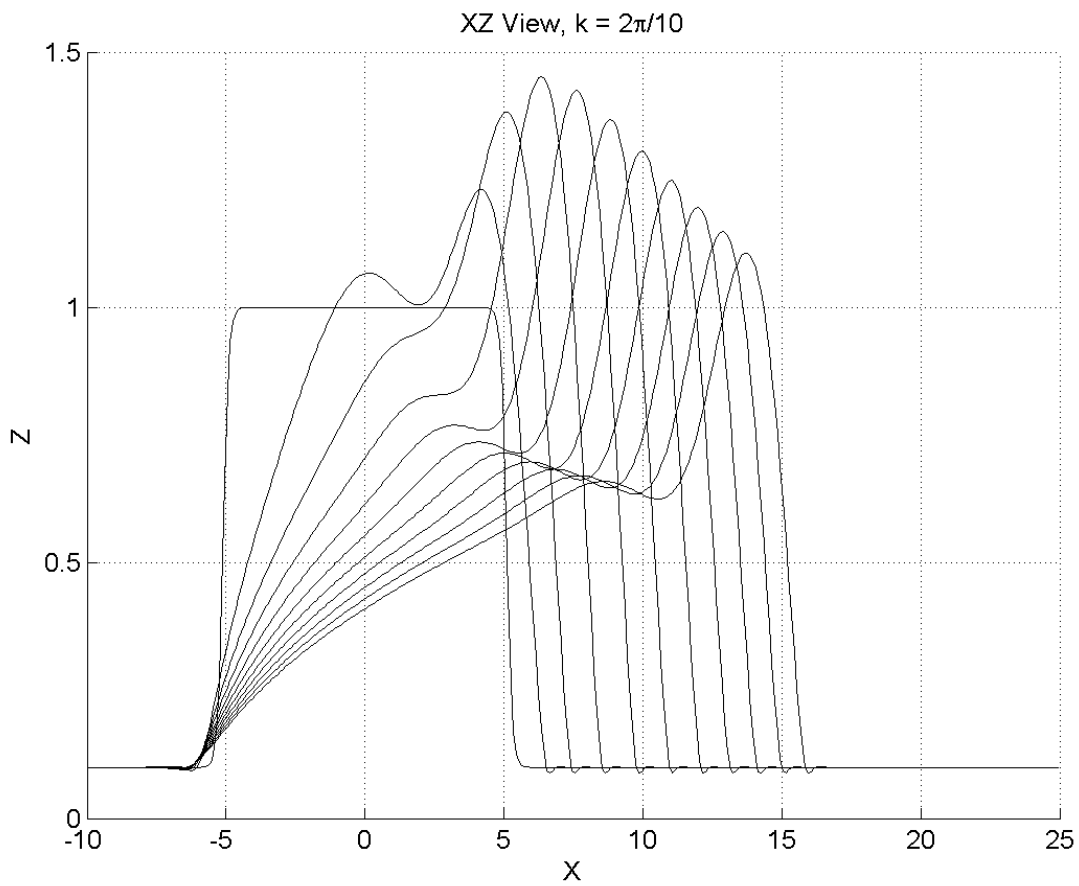
- [1] Diez, Javier A., and L. Kondic. "Computing Three-Dimensional Thin Film Flows Including Contact Lines." *Journal of Computational Physics* 183 (2002): 274-306. *Elsevier.com*. Elsevier Science. Web. 5 May 2011.
- [2] Kondic, L. "Instabilities in Gravity Driven Flow of Thin Fluid Films." *Society for Industrial and Applied Mathematics* 45 (2003): 95-115. *SIAM*. Web. 5 May 2011.
- [3] Witelski, T. P., and M. Bowen. "ADI Schemes for Higher-order Nonlinear Diffusion Equations." *Applied Numerical Mathematics* 45 (2003): 331-51. *Elsevier.com*. Elsevier Science. Web. 5 May 2011.

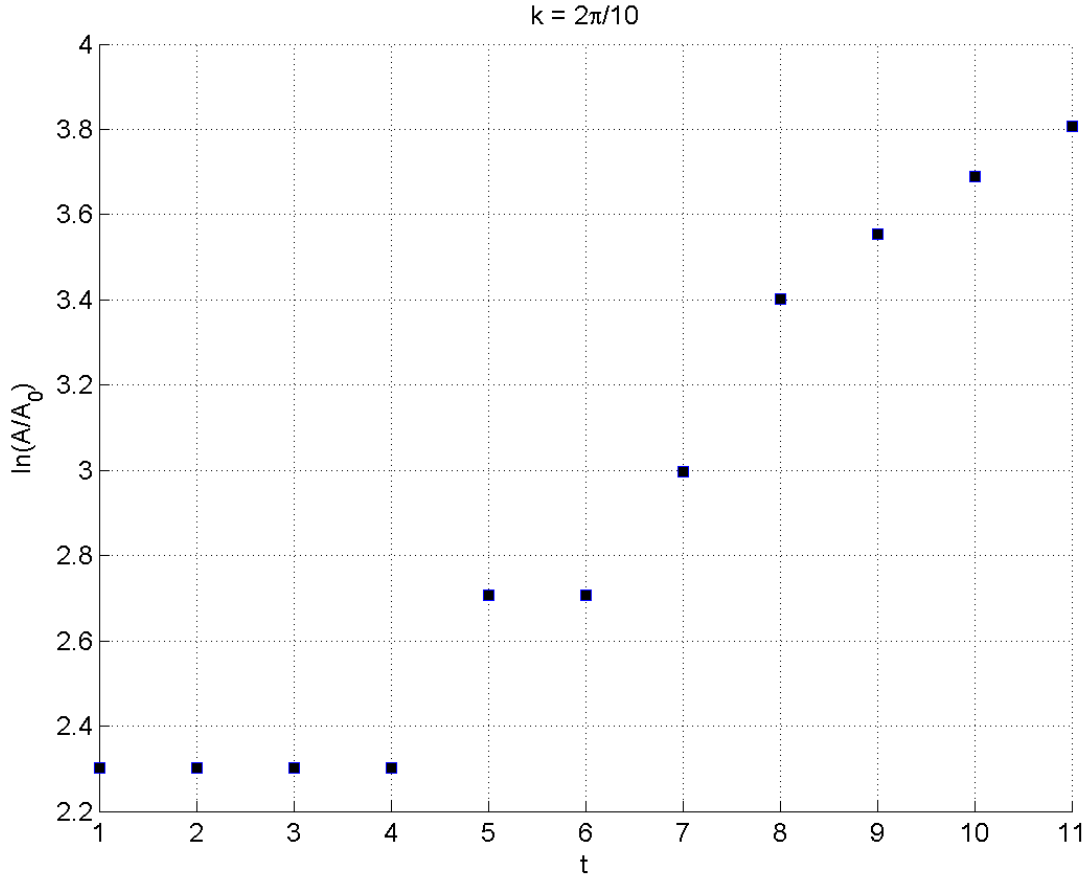
Growth Rate Analysis

Using linear stability analysis, we find that instability growth follows an exponential model ($A = A_0 e^{\sigma t}$). The technique to get this data follows:

All the simulations for this part (both constant volume and constant flux, for all different λ) were with parameters $c = 1$, $N = 10$, $u = 1$, and $B = 0$. This implies, these simulations are for flow down a vertical surface. All simulations were run until $t = 10$ and output files are created every 1 unit of time. The growth rate, σ , was obtained using a linear fit for the model:

$$\sigma t = \ln\left(\frac{A}{A_0}\right)$$





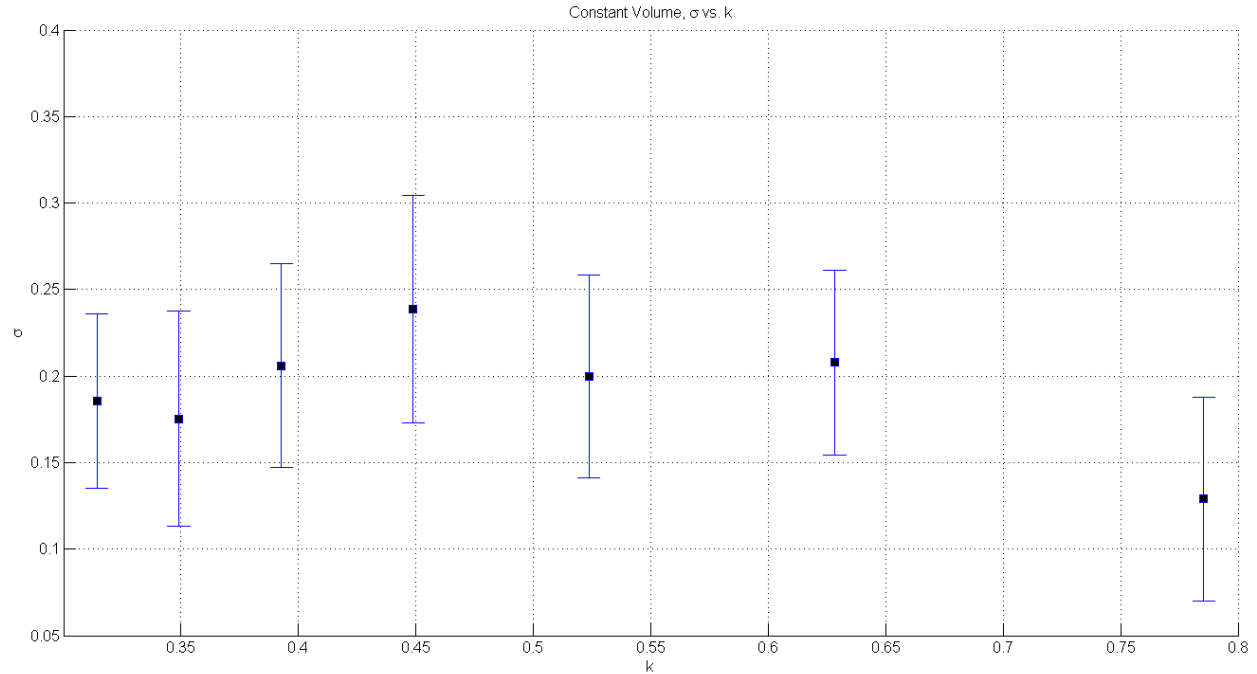
The A values were calculated by subtracting the minimum of XZ profile at $\frac{y}{2}$ (where we expect the middle of the wave front to be) and the XZ profile at $y = 0$. The

Below are the computed growth rate values with 95% confidence.

$$k = \frac{2\pi}{\lambda}$$

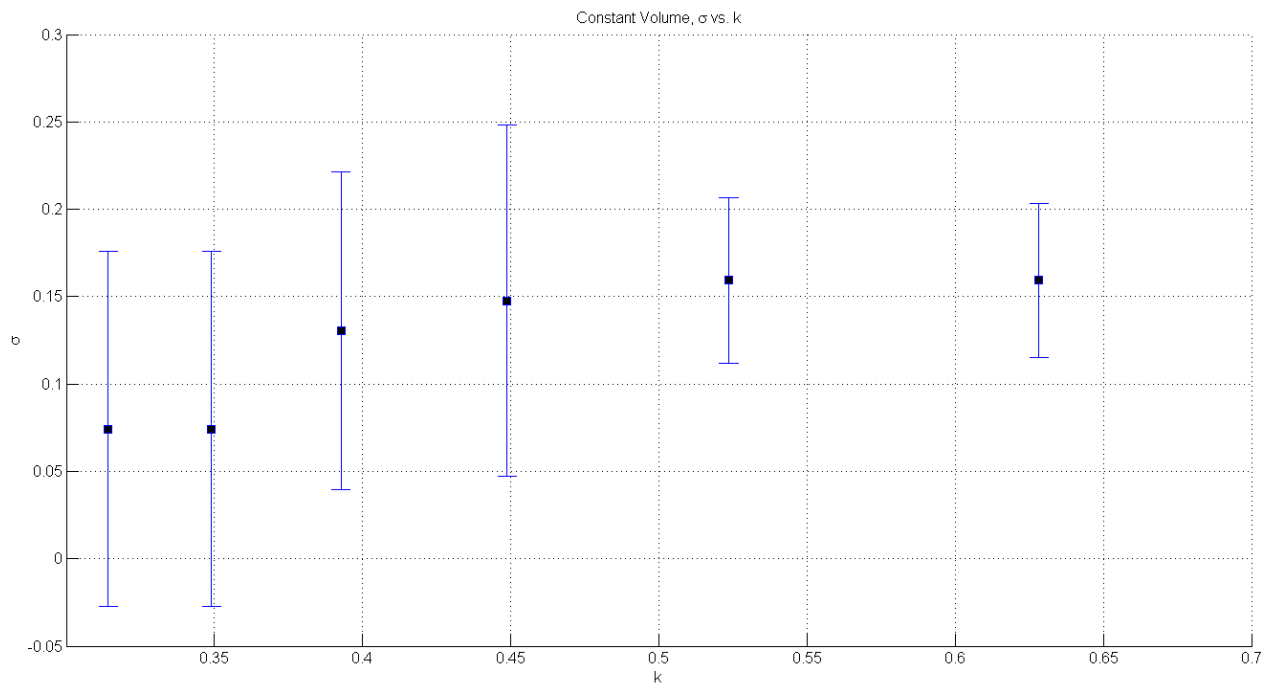
$\lambda = y_{max}$	k	σ (Constant Volume)	σ (Constant Flux)
8	0.7854	$\sigma = 0.129$ (0.07001, 0.188)	
10	0.6283	$\sigma = 0.2078$ (0.1544, 0.2611)	$\sigma = 0.1593$ (0.1152, 0.2033)
12	0.5236	$\sigma = 0.1998$ (0.141, 0.2585)	$\sigma = 0.1593$ (0.112, 0.2065)
14	0.4488	$\sigma = 0.2386$ (0.1728, 0.3043)	$\sigma = 0.1477$ (0.04715, 0.2482)
16	0.3927	$\sigma = 0.206$ (0.147, 0.2651)	$\sigma = 0.1305$ (0.03936, 0.2216)
18	0.3491	$\sigma = 0.1752$ (0.113, 0.2374)	$\sigma = 0.07427$ (-0.02718, 0.1757)
20	0.3142	$\sigma = 0.1855$ (0.1352, 0.2358)	$\sigma = 0.07427$ (-0.02718, 0.1757)

For constant volume, the calculated σ is:



Above plot shows the expected relationship between σ and t .

However, for constant flux, the error is very large.



The data obtained using the simulations did not exhibit exact behavior expected via LSA. Similar analysis was done in the SIAM paper, where the author used only the data until $t = 5$. Getting more output files from first few time units should give a better approximation for σ .

The comparison of the obtained data with experiment is not possible at the moment because no comparable data was obtained from the experiment.

References

- [1] Cummings, L. J., Lin, T.-S. and Kondic, L., Modeling and simulations of the spreading and destabilization of nematic drops, *Phys. Fluids* 23, 4 (2011)
- [2] Kondic, L. (2003). Instabilities in gravity driven flow of thin fluid films. *SIAM Review*, 45(1), 95-115.
- [3] Lin, T.-S., Kondic, L. (2010). Thin films flowing down inverted substrates: Two dimensional flow. *Physics of Fluids*, 22(5), 1-10.